Chapter 7
Preclinical Imaging in Oncology: Considerations and Recommendations for the Imaging Scientist

Daniel P. Bradley and Tim Wyant

Abstract Oncology remains a major focus of the pharmaceutical industry, and they are investing heavily in the forward effort to move drugs and biologics through development to regulatory approval. The discovery and early preclinical development throughput for safety, tumor cell binding, and in vivo biodistribution are hindered by the complications and the uniqueness of frequently contrived xenobiotic animal models, generally in murine strains. Animal numbers for adequate sensitivity, tumor heterogeneity of response, and metabolism make for high tumor-to-tumor variance in growth and response. The throughput of studies (tumor growth periods), powering studies sufficiently for decisional steps in product advancement, and the general "how do we do the human translation" all contribute to the major costs in this arm of the pharmaceutical business. Imaging offers many advantages to help solve, or at least allay, these issues. Imaging can pinpoint the tumor uptake heterogeneity, it can reduce the numbers of animals as quantitative assessments can be done on fewer animals, it allows for each animal to serve as its own control, and it allows multiple time point sampling in the same animal(s) during the tumor gestation, eruption, and time window for optimal therapeutic intervention. This chapter will hopefully guide the reader through multiple examples of how to investigate tumor biology using imaging in the nonclinical environment and hopefully will provide useful approaches and ideas for inclusion in their oncology programs.

D.P. Bradley, Ph.D. (✉) • T. Wyant, Ph.D.
Millennium: The Takeda Oncology Company, Cambridge, MA, USA
e-mail: Daniel.bradley@mpi.com

B.R. Moyer et al. (eds.), *Pharmaco-Imaging in Drug and Biologics Development*,
AAPS Advances in the Pharmaceutical Sciences Series 8, DOI 10.1007/978-1-4614-8247-5_7,

7.1 Introduction

Advances in targeted therapies in oncology have necessitated more specific biomarkers to be developed to aid in patient selection, targeted design, and prediction to response, e.g., biomarkers representative of pathway activation/inhibition such as KRAS, EGFR, ALK (Ou et al. 2012; Vincent et al. 2012), and cell-surface markers (CD30 for SGN35 and HER2 for Herceptin) (Zieba et al. 2012). Furthermore, as the hallmarks of cancer origin and in situ expression become better understood, new measurements and even new measurement tools for these oncologic hallmarks will be developed as they are uncovered (Hanahan and Weinberg 2011).

Biomarkers of oncology (and other areas as well) are typically identified as participating in a mechanism of action (MOA), or emerge as a result of the MOA, and thus are developed at the later discovery stage of a targeting new chemical entity (drug/biologic/tracer molecule) as a consequence of the target interaction. Once a drug–target interaction (binding or response) is recognized, the biomarker is rigorously tested and qualified (i.e., validated) in the context of a targeted therapy, i.e., regulatory approval directed efficacy and safety studies for testing in a phase 1 clinical trial. Pharmacodynamic biomarkers, which are often in the imaging realm, are typically used early in phase 1 and 2 trials. Response markers for a successful cancer therapeutic, e.g., tumor size reduction can be measured using CT or MR using criteria such as RECIST—Response Evaluation Criteria In Solid Tumors (see http://www.eortc.be/recist/). Tumor size reductions via product (test agent)-induced apoptosis/necrosis may encourage continued development of the product. Recent draft FDA guidance on the development of companion diagnostics (CDx; a diagnostic used to direct a specific therapy) recommends parallel development of the CDx from the time the need for a companion is identified and through the same registration trials being completed for the drug approval for the selected drug/biologic disease indication (in vivo (imaging) CDx, e.g., the FDA-approved Novartis' product Exjade® in the treatment of iron overload in non-transfusion dependant thalassemia (NTDT)). FerriScan®, an MR imaging agent, is used in studies to select patients for therapy and to manage their Exjade® therapy. FerriScan® provides the needed measure of liver iron concentration (LIC) necessary for Exjade's safe and effective use; see http://www.haemoglobin-gstt.org/images/14/127/ferriscan%20and%20monitoring%20forum%20may%2009.pdf.

Conventional biomarkers include those that are extracted from directly biopsied material, typically the tumor or surrogate tissue, e.g., associated supportive or co-localized tissues or plasma. Samples are subsequently analyzed with various diagnostic or other analytical techniques such as simple histology, immunohistochemistry, FISH (fluorescent in situ hybridization), and PCR and blotting techniques for detecting genetic change, mutational events, and aberrant protein expression.

One of the more promising current techniques developed to exploit biomarkers (physiologic as well as pharmacologic) is imaging. Imaging has long been used in clinical practice to assess solid tumor response to chemotherapy (e.g., RECIST using CT or MRI). However, the use of targeted imaging agents as probes

(e.g. EC20 for folate receptor imaging) or endogenous contrast (e.g., DWI or DCE-MRI) based upon tumor functionality has expanded the opportunity of using imaging platforms to address questions involving molecular responses as well as potentially screening patients for specific therapeutic regimens using biomarker selection strategies. Biomedical imaging sciences offers specific advantages to conventional biomarker assessment requiring interventional sampling. The capability of noninvasive measurements, longitudinal assessments, multiple lesion identity or discovery in the whole body, parametric mapping on individual tumors to extract info on therapeutic response heterogeneity, and the ability to capitulate on multiple clinical parameters extracted in one imaging session are major clinical improvements we have witnessed in clinical practice over the past few decades.[1] The nondestructive nature of imaging allows scientists and physicians to measure dynamic parameters associated with functional and intact systems, e.g., vascular hemodynamics and pathway activation/inhibition.

In addition to the above, imaging sciences offer a potential to address some of the challenges faced currently with companion diagnostics. For example, Knowles and Wu (2012) noted that the use of trastuzumab (an anti-HER2 therapeutic antibody) in patients is only 20–30 % effective in a subpopulation of HER2-positive breast cancer patients as determined by immunohistochemistry or fluorescent in situ hybridization at initial diagnosis. In the situation of breast cancer metastases, HER2 expression is only inferred from the primary lesion. Whole body imaging may in the future play a role in identifying patients with HER-positive metastases expressing differing levels of the HER2 target, and thus imaging may be able to predict favorable outcomes from use of expression-specific directed therapeutics.

One must be cognizant of the fact that no one biomarker is "king," and typically in drug development, a comprehensive and complimentary biomarker strategy is more likely necessary to predict therapeutic success and accelerate development. The clinical goal is to improve probability of success in the selection of the appropriate therapy for the discovered oncologic expression and in the appropriate patient. Indeed, as the reader moves through this chapter, they must always consider the reproducibility and validation of the imaging technique in the context of the clinically relevant animal models that best mimic the human cancer in question, dose of the therapeutic and the reporter CDx, timing of image acquisitions during disease progression and treatment to indicate treatment success (or failure), and quantitation of the benefits (or lack thereof) and risks (if known) of pharmacological intervention.

Again, biomedical imaging has long been used in patient management in oncology. Anatomical or structural scanning, where a dimension or dimensions of target lesions are measured with of the utility of the World Health Organization's (WHO) RECIST1.0 (http://www.recist.com/) using CT or MR imaging (and now RECIST1.1 (and soon Positron Emission Response Criteria in Solid Tumors PERCIST using PET technologies)), which allows for quantitative response measurements via solid tumor size changes. However, more recently with the advent of targeted therapies, tumor imaging techniques have stepped into a new, and potentially very large,

[1] For example, FDG-PET and CT, MRI (DWI and MRS).

territory where we have novel functional or molecular uptake/washout readouts. Definitions were recently described at the Society of Nuclear Medicine 2010. This international body of nuclear imaging scientists and physicians was recently renamed as SNM Molecular Imaging, or SNMMI, partly in recognition of the expansive growth of nuclear medicine and its armament of novel molecular imaging agents (now including nonnuclear optical imaging), quantitative image processing computational systems, and the wide expanse of research activities including:

- *Molecular imaging agents*: "Probes" used to visualize, characterize, and quantitate biological processes in living systems. Both endogenous molecules and exogenous probes can serve as molecular imaging agents.
- *Molecular imaging instrumentation*: The platform technologies that "comprises tools that enable visualization and quantification in space and over time of signals from molecular imaging agents."
- *Molecular imaging quantification*: The science of computational determination of regional concentrations of molecular imaging agents and biological rate constants/pharmacokinetic/pharmacodynamic parameters. Further, molecular imaging quantification provides measurements of processes acting at molecular and cellular levels. Quantification is a key element of molecular imaging requiring a clear understanding on the origin of data and the limitations as well as the expectations of image analyses, especially as we control for inter- and intrasubject comparisons.

Describing these three listed elements in full goes well beyond the scope of this chapter, but the reader should explore other chapters in this volume where they may find information on molecular imaging platforms not included in this treatise including DCE-MRI (dynamic contrast enhanced-MRI) and DCE-CT for antiangiogenics, fluorodeoxyglucose PET (FDG-PET) in glycolytic-targeted therapies, and Octreoscan for somatostatin receptor participation in cancer physiology (Velikyan et al. 2010). A recent review examines the role of functional and molecular imaging in predicting response to specific therapies (Morse and Gillies 2010), and more advanced MI techniques are described by Pysz et al. (2010).

As we review biomedical imaging in the context of preclinical oncology models, it is important to consider and research the cohabitation of imaging probes that are also useful in other clinical endpoints, particularly in non-oncology disease areas, e.g., FDG-PET used in heart disease, atherosclerosis, and Alzheimer's research and DCE-MRI used in arthritis and inflammatory diseases.

This chapter will introduce the reader to small animal imaging technologies and techniques typically useful for oncology research and will attempt to expound on the techniques embedded in translational principles. Biomedical imaging research labs are becoming major partners with oncology research units across academic and pharmaceutical industry sites. Some reference will also be made to those novel agents used in MRI, PET, SPECT, US, and other platforms, but we will not cover the complex chemistry involved in the generation of these conventional and novel products. We recommend for a treatise on nuclear medicine applicable pharmaceuticals, the fine work written by Vallabahajosula ("Molecular Imaging: Radiopharmaceuticals for PET and SPECT"; Springer 2009; http://www.springer.com/medicine/nuclear+medicine/

book/978-3-540-76734-3) and for MRI contrast agents the treatise by Yim et al. (2011) ("Review Article: MRI Contrast Agent-Based Multifunctional Materials: Diagnosis and Therapy"; Journal of Nanomaterials, 2011, Article ID 747196, 11 pg; http://www.hindawi.com/journals/jnm/2011/747196/). For ultrasound (US) contrast agents, please refer to the ACR Guidelines: ACR Manual on Contrast Media, 8, 2012; ACR Committee on Drugs and Contrast Media, http://www.acr.org/~/media/ACR/Documents/PDF/QualitySafety/Resources/Contrast%20Manual/FullManual.pdf.

This chapter will examine several techniques that can be reasonably used within several models of interest in oncology. Finally, while many methods exist to measure similar biological and pharmacological processes, some techniques are simply better suited than others (e.g., DCE-MRI vs. DCE-CT where the former lacks the risk of the absorbed dose from ionizing radiation using radio waves alone as the means of image signal collection).

7.2 Animal Models: Use and Preparation

The most common species used in preclinical oncology is the immunocompromised mouse. This model includes strains such as the nude (nu/nu), SCID, and NOD-SCID mouse (Firestone 2010). The selection of choice of the use of a specific strain can be dictated by many factors and resources exist that have updated their comprehensive lists of the different models and their protocol-desirable characteristics, e.g., http://cancermodels.nci.nih.gov/camod/. The immunocompromised background of these strains necessitates meticulous protocols to limit the exposure of animals to environmental factors that could compromise their general well-being and risk of nosocomial infections. As such, appropriate personal protective equipment and good lab practice is to be followed to reduce inherent risks to the animals. Not all imaging labs can perform under controlled environments or operate in a "barriered" facilities and the incorporation of such skill sets involves extensive training and equipment (there are exceptions, e.g., MI http://molecularimaging.com/) (Note: For a complete treatise on imaging facilities for infection studies with Select Agents, please see Chap. 10 (Keith et al.) where the reader can be introduced to imaging in BSL-3/4 facilities and the details of these imaging procedures).

While preclinical imaging technologies generally share the same engineering and physics principles as its clinical counterpart, in almost all cases small animal subjects have to be immobilized via inhalational and/or injectable anesthetics. With anesthesia, the operator must consider physiological monitoring to ensure appropriate depth of anesthesia and in the case of PET, SPECT, MRI, or Optical to allow for the collection of data in a manner that may allow for gated (physiologic event triggered) acquisition. Multimodal data capture can be improved by integrated bed design as demonstrated by Nelson et al. (2011), to allow registration of images collected using different axial modalities especially when images are not collected in the same gantry. Cradle or "sled" systems that incorporate ECG, respiration, and temperature monitoring sensors are now used in a preclinical setup (Fig. 7.1a) in conjunction with the use of appropriate and validated monitoring instrumentation (Fig. 7.1b).

Fig. 7.1 (**a**) DAZAI system where specific beds are molded to mice of differing body weights and the resulting "sled" is fitted with ECG, respiration, and thermocouple sensors for full physiological monitoring of an animal's well-being while under anesthesia. (**b**) SAII system integrated with the DAZAI system, the SAII monitoring hardware allows the physiological signals to be electronically traced and stored; furthermore, integrating this system into the MRI or PET hardware enables the operator to gate/trigger acquisitions to cardiac and/or respiration cycles

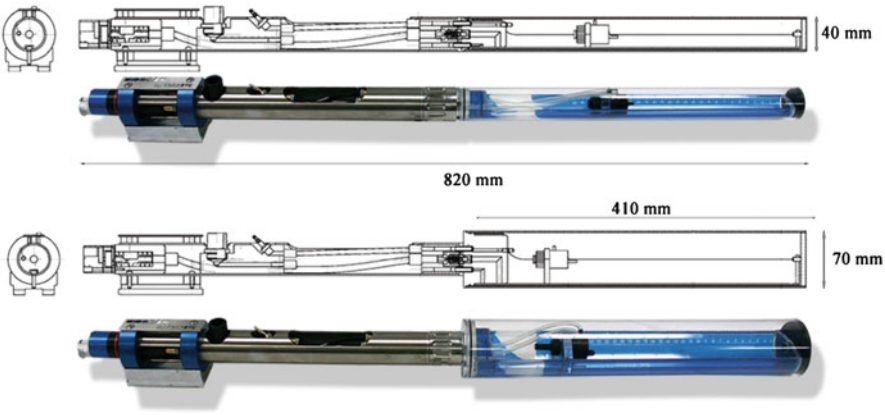

Fig. 7.2 Examples of the tubular designs that are for animal holding and "insertion" via a contained environment into an imaging system. These are applicable to small as well as large animals. Also, see Chap. 10 on BSL-3/4 laboratory imaging requirements

Other systems exist that permit use in either barriered or non-barriered facilities, e.g., bioscan-barriered cradles (Fig. 7.2). Such systems permit the transfer of animals from barriered facilities into "dirty" (i.e., uncontrolled or allowed to be contaminated) imaging platforms/imaging labs, all the while limiting the animal and animal handlers exposure to pathogens.

Where anesthesia is not appropriate and yet immobilization is preferred, there are instances where rats have been habituated to scanner systems and complex cradle designs can be of assistance. However, most animals are typically restrained while conscious using ear and mouth bars and/or body harnesses (Ferris et al. 2011). The appeal of conscious imaging has primarily been driven by the need for "awake" conditions for functional MRI (fMRI) and pharmacological stimulated MRI (phMRI)[2] communities where functional MRI uses blood oxygenation level dependent (BOLD) blood flow responses to measure regional blood flow changes due to imposed stimuli. BOLD responses can often be attenuated/altered by anesthetics (Hodkinson et al. 2012). A limited number of oncology studies have explored the effects of anesthesia on basal physiological measurements using MRI (Baudelet and Gallez 2004) and bioluminescence (Schnell et al. 2010) in rats with xenograft tumors. In experimental design it is typical to have a size and time matched control

[2] fMRI (functional magnetic resonance imaging) relies on the hemodynamic response and exploits the magnetic susceptibility differences between hemoglobin in its two different oxygenation states (deoxy- and oxyhemoglobin), and during neuronal activation there is a vascular response associated that can "flood" the neural region with oxygenated blood and increase the signal measured on T2* weighted imaging—this activation can come about from visual, motor, physiological stimuli. phMRI (or pharmacological MRI) uses the same imaging technique, but instead of an environmental stimuli, the subject receives a pharmacological stimulus that is thought to activates/inhibits brain centers.

or vehicle arm to understand the impact of the procedure on the "control" parameters being examined. However, careful consideration must be made when studying biological processes under different anesthetic states (Kersemans et al. 2011a). Anesthetic usage under conditions of animal termination (or non-recovery) may be done, but limits of duration may be governed under local animal license authorities, and consultation with these authorities should be considered when designing your studies. The authorities often will allow for longer scan times in these cases (1–2 h); however, in recovery-directed procedures where the animal will regain consciousness after the scan, careful consideration and ethical approval has to be sought when scanning with recovery. Furthermore the frequency of scanning and number of times each animal is exposed to anesthesia (and ionizing radiation in the case of PET and CT (see below)) has to be carefully considered when designing longitudinal studies; thus while "using each animal as its own control" is often cited as a great advantage of noninvasive imaging if that animal is under stress and not eating, grooming, or out of sync in its sleep–wake cycle, the data recovered from each scan and noise added could get progressively worse and be unreproducible and unreliable.

7.2.1 Major Modalities Used in Preclinical Oncology Drug Discovery: Principles, Limitations, and Applications

Many biomedical imaging laboratories exit in universities and pharmaceutical companies as core or central labs, and some exist within disease area departments (e.g., neurology, oncology, cardiovascular). Institutions without such facilities often exploit the small animal imaging CROs that exist across the globe. However, integrated imaging facilities have the advantage of exploiting proprietary novel animal models and procedures, unhindered access to different supportive functions (e.g., DMPK, molecular pathology, histology, chemistry, pharmacology, toxicology) and novel therapies being developed. Below, a number of the key translational modalities will be described, and examples in the oncology setting will be presented. Magnetic resonance imaging, positron emission tomography, and single photon emission computed tomography will be described. Firstly, MRI typically exploits the endogenous contrast brought about by the magnetic properties of the proton residing in H_2O—multiparametric acquisitions are one of the greatest benefits of MRI, plus non-ionizing radiation. MRI offers exquisite spatial resolution for anatomical imaging and more advanced uses now allow the measurement of many different physiological events in normal and diseased tissues. Second, PET relies on the administration of a positron-emitting isotope typically attached to a small molecule or via chelation on to larger molecules. While ^{18}F- FDG remains the cornerstone of oncologic PET examinations, more "boutique" isotopes are making inroads due to both ready complexation with common chelators (e.g., ^{68}Ga and DOTA, DTPA) and independence from cyclotron infrastructure. Finally SPECT, like PET, relies on gamma-emitting isotopes but instead detects the emissions directly (rather than through the annihilation process as in PET). Similarly, radiolabeled probes are

used that are either nonspecific (e.g., blood flow using Tc-99m hexamethylpropyleneamine oxime (Tc-99m HMPAO)), absorbed by certain cell types (e.g., bone uptake using Tc-99m methylene diphosphonate), or a targeted to specific cell-surface markers (e.g., ^{111}In trastuzumab). All these modalities will be described in more detail below.

7.2.1.1 Magnetic Resonance Imaging (MRI)

Often referred to as a "conventional anatomical imaging" procedure, magnetic resonance imaging (MRI; formerly termed nuclear magnetic resonance, NMR) provides exquisite soft tissue contrast without exposing the subject to harmful ionizing radiation. However, many "functional" and "molecular" MRI techniques exist including those that measure changes associated with hemodynamic responses in fMRI and antiangiogenic treatments in oncology, to metabolic profiling of spatially distinct regions of tumors (magnetic resonance spectroscopy (MRS)) and the onset of cell death during stroke or cytotoxic therapies to name but a few—methods successfully used in clinical and nonclinical subjects.

The body is made up largely of water molecules (H_2O), and it is the hydrogen atoms of the water molecules that possess a property exploited under high magnetic fields, e.g., the atom is essentially a magnet with a positive pole (the nucleus or singular proton) and a negative pole (the singular electron). The odd number of protons, ^{1}H, presents with a nonzero spin that results in NMR properties. In an applied magnetic field, B_0, two spin states arise (high and low energy) and transition between these two energy states can be induced by absorption of electromagnetic energy (B_1) generated by a radiofrequency (RF) coil at a specified frequency unique to the nuclei under investigation.[3] After excitation there is a loss of energy termed "relaxation" and this loss is governed by specific properties of the sample. The loss from relaxation is measured by the same or separate RF coil proximal to the sample. Longitudinal (T1) relaxation is the process by which the spin system returns to equilibrium state releasing energy back into its surrounding environment or "lattics" after the removal of the B_1 field. Transverse or spin–spin (T2) relaxation describes the rate of which the spins diphase due to inter- and intramolecular interactions after B_1 has been turned off. During the excitation period a series of additional magnetic fields which form a "gradient" through the sample and thus when applied creates an encoded spatial relationship of the signals and allows the operator to utilize spatially unique volumes to provide their own respective relaxation energy loss. This information created by manipulation of the RF power, timing (single or repeated application), shape, and duration of the RF and gradient pulses gives rise to the different "weighting" of volume elements within an MRI image. For a review of MR imaging

[3] It is not just 1H-containing molecules that can be studied with MRI but also the elements of P, C, N, Na, F, etc.

in the mouse using a variety of MR pulse sequences and methods, the reader is directed to Pautler (2004).

Small animal MRI systems from 1.5 to 17 Tesla (T; SI term of magnetic field strength) have been used for a variety of study objectives; the higher the Tesla (B_0), the greater the signal to noise ratio (SNR)—however, as field increases so does the size of the physical laboratory footprint of the system. Most preclinical systems lie in the range of 4.7 T (200 MHz)–9.4 T (400 MHz)—lower field systems can be more advantageous when imaging T1 and T2 signals. Susceptibility artifacts or noise introduced by small RF-induced susceptibility relaxation loss of hydrogens associated with nonspecific molecular entities can also be a problem at higher field (refer to Chap. 11 (Moyer, Hu and Williams) for a short treatise on the MRI operational physics and their controls).

The major advantage of MRI is the ability to acquire multiple contrast endpoints in a single imaging session, and this can be done with no injection of exogenous agents. For example, T1, T2, ADC (apparent diffusion coefficient), and MRS data can all be acquired in a single imaging session of a target lesion. Other advantages include the avoidance of ionizing as used by CT, SPECT, and PET where ionizing radiation provided their interpretive signal. Thus, MRI use provides multiple imaging sessions without deleterious absorbed ionizing radiation to the subject. Additionally, hardware can be modified to improve SNR (signal to noise ratio) and temporal resolution. For the former, this can be accomplished using different RF coil configurations termed volumetric, surface, or phased array (Doty et al. 2007), and cryo-cooled RF (B_1) systems are available by different vendors and custom-built in engineering laboratories. Finally, multiple nuclei of interest can be measured using decoupled RF coils tuned to the respective resonant frequency of the targeted nuclei, e.g., ^{1}H for lactate and ^{31}P for ATP measurements, respectively.

MRI has historically been reserved for the physicist applying their knowledge in a biological context; many vendors offer customized acquisition routines to trigger relaxation losses of specific targeted tissues or molecular entities that need to be optimized on site, and this requires pulse sequence coding and an in-depth knowledge of MRI physics. However, more vendors are releasing user friendly and ”target-ready” acquisition routines for high-throughput imaging of genetically engineered murine models using standard MRI parameters, e.g., T1W (T1-weighted) or T2W (T2-weighted) imaging. Preclinical imaging vendors are also offering systems with clinical operating systems to aid in translation of imaging techniques from the animal model laboratory to the clinical bedside. Furthermore, some of the newer systems even negate the need for dedicated areas of operation. For example, most high field superconducting magnets weigh more than 6–10 K pounds and possess a “stray field” that limits the proximity for monitoring equipment (i.e., cardiovascular system measuring devices such as ECGs) and other electronic devices (phones, watches, and other nonexperimental associated devices). Newer systems, are lighter and can be even described as benchtop devices (however, these are currently limited to 0.5–1 T) and can be applied when high-throughput genotyping of genetically engineered mouse models or chronic disease measurements are required for example. These smaller and lighter systems and potentially “open” systems (most

are ring systems that can be claustrophobic in clinical settings) also some do not require cryogenic cooling, i.e., repeated filling with liquid nitrogen (e.g., those produced by http://www.mrsolutions.co.uk/products/benchtop/).

Physiological, physical, and hardware-associated artifacts can often compromise the quality of MRI data and thus affect the fidelity and clinical interpretations of mathematically reconstructed images. While not to concern the new user of MRI, there are many type of artifacts that can be attributed to different sources. Some examples are listed in http://www.mritutor.org/mritutor/artifact.htm/, and this chapter cannot detail all of these (refer to Chap. 11 (Moyer, Hu, Williams and Morris) in this book and also see Smith and Nayak 2010).

Many scientific publications provide good examples of how MRI has been used in preclinical models of oncology; the simplest applications of MRI are when it is used as a tool for identifying lesion location, size, volume, and morphology, i.e., anatomical criteria. However, more advanced acquisition examples include those that acquire multiparametric maps to either determine basal differences between tumors of a different genotype or detect acute changes in the tumor physiology following drug action.

Considerations on small animal imaging in a recent and comprehensive review (Barnes et al. 2012) on dynamic contrast enhanced-MRI (DCE-MRI) can easily translate across different modalities. DCE-MRI is applicable when one wishes to study therapeutic agents that target the vasculature, but it also has value when studying imaging endpoints that rely on tracer delivery. For example, PET requires the administration of a labeled molecule and typically this molecule is trapped through an enzymatic reaction leading to metabolic stasis (e.g., ^{18}F FDG and the hexokinase failure to metabolize the deoxy form of glucose leading to the drug being "static" in situ allowing for image acquisition) or binds to a surface antigen (e.g., ^{89}Zr-Herceptin). For both of these examples, the drugs are delivered via the vasculature and the fractional delivery over time to the tumors (termed the "input function") allows mathematical measures and a way to understand those factors important in affecting tracer uptake. Measurements of the vasculature fractional distribution can be made with specific vascular agents (e.g., Gd-DTPA) or surrogate measurements can be derived from dynamic acquisitions of the targeted tracer. Different hemodynamic constituents associated vascular perfusion, vascular volume, vascular permeability and intra- and extravascular compartments can be extracted from DCE-MRI with different compartmental modeling routines (McGrath et al. 2009).

Diffusion-weighted MRI (DWI) exploits the endogenous diffusion properties of H_2O; in principle and in the context of oncologic endpoints, the assumption is based on the two major compartments in the microenvironment of a tumor having different diffusional properties, the extra- and intracellular space (ECS and ICS, respectively). Indeed, on induction of cell death, through apoptosis or necrosis, the change in the ratio of the two compartments can lead to a dramatic change in water diffusion paths, and this can be detected using DWI and be predictive for tumor shrinkage (Heijmen et al. 2013). For a comprehensive review of DWI applications and concepts, see Neil (2008) and Padhani et al. (2009).

While not "imaging" per se, magnetic resonance spectroscopy (MRS) exploits the NMR properties of spinning nuclei (for a full treatise on MRS-applications in

imaging, see Chap. 12 by Venter et al. in this volume). With the advent of metabolomics (the global quantitative assessment of endogenous metabolites within a biological system), noninvasive assessment of the cancer metabolome (inherent in situ metabolism and catabolism) is emerging as a powerful tool to measure this feature during disease progression, differentiating between benign and malignant lesions, and changes associated with tumor metabolism resulting from applied targeted therapies (Serkova et al. 2007; Spratlin et al. 2009). For a more detailed review of these imaging approaches and the importance of other factors affecting MRI image interpretations in basic preclinical research, see Albanese et al. (2012).

7.2.1.2 Positron Emission (Computed) Tomography (PET)

A compound labeled with a positron-emitting radionuclide, i.e., ^{11}C, ^{13}N, ^{15}O, ^{18}F, ^{64}Cu, and ^{82}Rb, is introduced into the body, usually by intravenous injection, to facilitate a rapid and high fractional dose input function to the desired anatomical target. When one of the radionuclide atoms decays, a positron is emitted from the nucleus and travels a very short distance and is annihilated with interaction with an electron resulting in the formation of two gamma rays. The mass of the two annihilating particles is converted into gamma energy forming two 511 keV gamma rays which oppose each other directionally by 180°. A positron emission tomography scanner consists of a ring, or multiple rings, of gamma-ray detectors that register coincident gamma ray "hits" in specific timing windows to define the near location of their origin in the body via a chord construct across the ring. By collecting large numbers of gamma-ray pair/coincident events (typically 10^6–10^7) and using computed tomography chord reconstruction methods, transverse cross-sectional images of the original 3D volume (a patient or a test animal) can be created. The frequency of chord crossover saturation points reflects the concentration of the positron-emitting radionuclide in the body slice as defined by the ring detector number, event resolution, and correction of photonic attenuation. For other detailed PET systems applications see Chaps. 2, 3, 4, 8, and 10 and also Jones (1996).

Advantages of PET, versus other imaging modalities in small animal cancer studies, are in its quantitative nature and very high sensitivity. The versatility for radiolabeling small molecules with PET radiotracers, including therapeutic agents (Bahce et al. 2013), is rapidly emerging as a tool that can be used to noninvasively assess whole body pharmacokinetic (PK) and pharmacodynamic (PD) parameters and can be used whether or not the level of tracer uptake corresponds to or depends upon the presence of activating tumor receptor mutations. Commonly used isotopes in PET are typically short-lived (minutes to hours), e.g., ^{18}F, ^{68}Ga, ^{11}C, and ^{15}O. However, the introduction of ^{64}Cu and ^{89}Zr as a longer-lived positron-emitting radioisotopes (half-lives of 12.7 and 78.4 h, resp.) that can be chelated and conjugated to Ab's has changed evaluation methods for Ab therapeutics. Antibody therapeutics typically exhibit long-lived biologic half-lives (re., PK), and they can now be labeled and imaged in both animal and human systems under conditions to measure their pharmacokinetic changes and the pharmacodynamic changes resulting in

their tumor-specific targets (Verel et al. 2003). Furthermore, where methods have been established using long-lived SPECT radioisotopes (e.g., ^{111}In and Tc-99m), positron emitters are slowly making inroads into the "hours post injection" territory currently favored using SPECT due to the improved PET radiochemistry with ^{89}Zr the more quantitative nature of PET.

^{111}In -DOTATOC, a somatostatin receptor (SSTR) ligand, has long been used for studying neuroendocrine tumors using SPECT. Emerging data suggests SST analogs labeled with ^{68}Ga as a PET radiotracer offers improved specificity and sensitivity (Buchmann et al. 2007). Preclinical evidence continues to emerge for ^{68}Ga as PET tracer demonstrating acceptable chelation chemistry (i.e., high specific radioactivity with limited radiolysis) allowing longer imaging and ability to reveal biological properties of targeted tissues (Breeman et al. 2011).

Preclinical examples of PET in cancer research are spread across radiolabeled small molecules, pathway targeted agents, antibodies, antibody fragments, and peptides (Aboagye 2005). A number of papers are highlighted below.

FDG-PET and other tracers have been evaluated in multiple tumors for general characterizing of target receptor avidity to the tracer (Kd or binding constants; Hill plots) or physiologic uptake (SUV or standard uptake value) and to measure the tracer kinetics in the context of acute therapeutic treatment (tumor apoptosis, shrinkage, etc.):

$$\mathrm{SUV} = r / (a' / w),$$

where r is the radioactivity activity concentration (kBq/ml) measured by the PET scanner within a region of interest (ROI), a' is the decay-corrected amount of injected radiolabeled FDG (kBq), and w is the weight of the patient (g) (Kinahan and Fletcher 2010).

For example, F-18 FDG, F-18 FLT, 18F-18 FET, and F-18FCH SUVs were evaluated in the recent paper by Ebenhan et al. (Ebenhan et al. 2009) and correlating the imaging data with tumor dissection, histology, and immunohistochemistry analysis of Ki67 (a marker of proliferation), Proliferating Cell Nuclear Antigen (PCNA), and Caspase-3. Some of the conclusions and highlights of this work are captured thus:

- Low and heterogeneous tracer uptake in experimental tumors represents a complicating factor for proper PET data interpretation.
- ^{18}F FDG imaging gives low tumor and low tumor edge (typically the metabolically active invasive border) tracer uptake, especially in human tumor xenografts in murine models.
- The murine models with the highest ^{18}F FDG uptake for the syngeneic orthotopic group (B16/BL6 strains) or SC (subcutaneous) xenograft group (U87 MG) showed the lowest ^{18}F FLT (fluorothymidine, a DNA targeting tracer) uptake for that group.
- ^{18}F FLT imaging appeared to provide the best imaging parameters (signal to noise) across all models.
- The correlation of ^{18}F FLT uptake with the proliferation markers Ki67 or PCNA was, however, relatively weak.

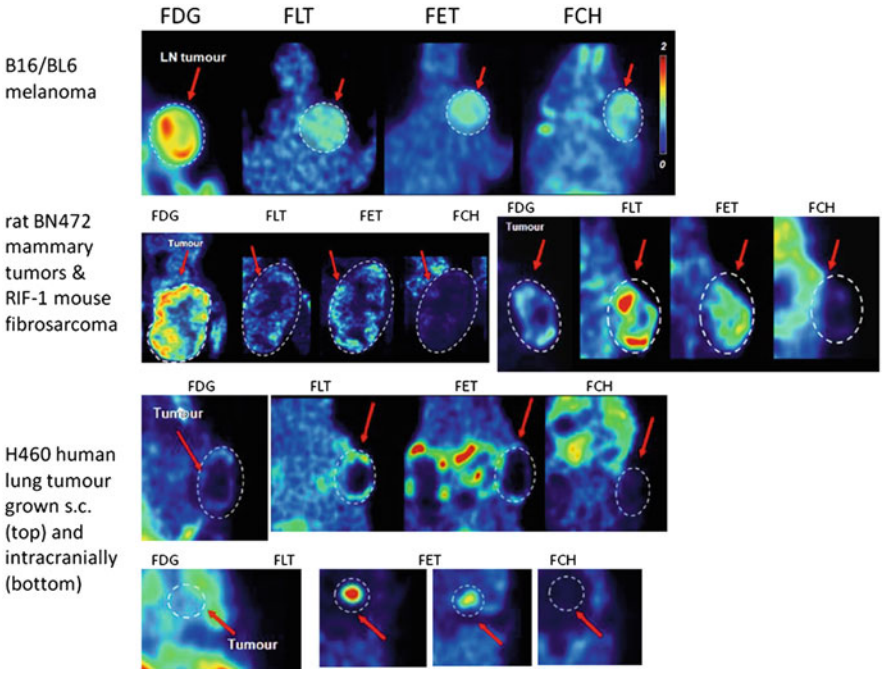

Fig. 7.3 Different tumor types and their avidity for different PET tracers (extracted and modified from Ebenhan et al. (2009); with permission)

- A very strong correlation between ^{18}F FLT uptake and tumor caspase-3 expression was observed (Fig. 7.3).

As is well known from the clinical setting, tumor response evaluated using the traditional RECIST (Response Evaluation Criteria in Solid Tumors; Therasse et al. 2006) alone is limited because many tyrosine kinase inhibitors (TKIs) do not lead to a detectable or statistical lesion shrinkage when first evaluated in small patient cohorts designed into a phase 1 clinical trial. Emerging preclinical FDG-PET, and clinical studies as well (McArthur et al. 2012), has demonstrated, in the context of novel targeted therapies, that modulating pathways associated with glycolysis can be used as an acute PD marker or one that also predicts for radiological outcome (Nguyen et al. 2011; Pantaleo et al. 2010). As with other modalities, when investigating imaging endpoints using preclinical models, central necrosis of solid tumors can confound therapeutic drug outcome results and careful consideration must be made on the mode of analysis or stipulate the starting size and rate of growth of tumors that are to be studied.

Complex chemical synthetic paths for radiolabeling with ^{11}C and the short half-life of ^{11}C have limited the utility of this tracer in imaging of therapeutic molecules. However, recent improvements in the radiochemistry have increased this tracer use. For example, erlotinib can be labeled with ^{11}C (Memon et al. 2009) and examined

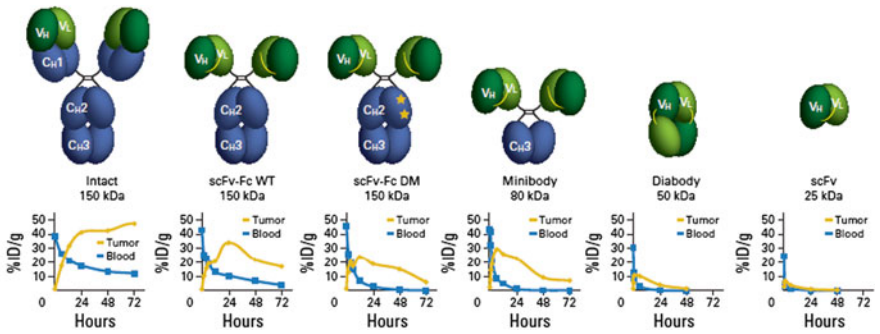

Fig. 7.4 Examples of changes in pharmacokinetic patterns that may occur with changes in antibody structure. The half-lives of immuno-PET imaging agents can be modified by (1) deleting constant domains to create fragments of varying size (single-chain Fv [scFv]-Fc, minibody, and diabody) or (2) by mutations that modify interactions with the FcRn receptor (scFv-Fc H310A/H435Q double mutant [DM]). For intact antibodies, imaging at 96–168 h provides optimal contrast. Antibody fragments such as scFv-Fc wild type (WT; 72–120 h), scFv-Fc DM (12–48 h), minibodies (8–48 h), and diabodies (4–8 h) are capable of obtaining high-contrast images at earlier time points (From Knowles and Wu (2012); with permission)

in multiple cell lines in vivo with different levels of EGFR expression and activity. Dynamic micro-PET has showed that HCC827 tumors have higher ^{11}C erlotinib uptake and retain the radioactivity significantly longer as compared with A549 and NCI358 tumors. However, the target tumor %ID/g is still relatively low (max uptake of 3.7 %ID; percent of injected dose). These results though have led to the quantitative measure of ^{11}C erlotinib uptake in patients with non-small cell lung carcinoma (NSCC) and found that it was significantly higher in tumors with EGFR-activating mutations (Bahce et al. 2013).

The more favorable PET radiotracer, ^{18}F, has a longer half-life (2 h vs. 20 min for ^{11}C) and also has complex radiochemistry for erlotinib, but the final step is the addition of F-18 which has advantages of specific activity but simply does not have a high enough yield for imaging. Ritter's group at Harvard, however, have improved the design and synthesis of an organometallic complex made from fluoride that behaves as an electrophilic fluorination reagent, and the use of the reagent for the synthesis of F-18-labeled small molecules via late-stage fluorination has been a breakthrough for high specific activity yields (Lee et al. 2011a).

Immune-positron emission tomography (immune-PET), i.e., imaging with intact antibodies, has shown success clinically in diagnosing and staging cancer. Engineered antibody fragments, such as "diabodies," "minibodies," and single-chain Fv (scFv)-Fc fragments, have been successfully employed for immune-PET imaging of cancer cell-surface biomarkers in preclinical models and are poised to bring same-day imaging into clinical development due to clearance kinetics (Knowles and Wu 2012) (Fig. 7.4).

7.2.1.3 Single Photon Emission Computed Tomography (SPECT)

For the physics of SPECT, the reader is referred to Groch and Erwin (2000), and in the context of small animal imaging and SPECT, see Franc et al. (2008) and Seo et al. (2013). Briefly, SPECT measures γ-rays directly after radionuclide emission, thereby gaining a theoretical advantage in spatial resolution over PET, for which resolution is currently limited by the fundamental processes of positron emission and positron–electron annihilation which occur away from the actual nuclear site of origin of the positron. SPECT uses many radiopharmaceuticals which are widely applied in clinical nuclear medicine and often have longer half-lives than most PET isotopes and therefore can be obtained from central radiopharmacies. Small animal SPECT studies generally cost less than other small animal imaging methods, such as small animal PET or small animal MRI. However, in contrast to PET the attenuation of detectable photons by soft tissue is estimated to be up to 50 % when imaging I-125 and up to 25 % when imaging Tc-99m in "rat-sized" objects thus leading to a potential decrease in the targeting sensitivity.

The main reasons for the advantage of SPECT, compared with PET, in brain imaging are the ability to push the spatial resolution to below 1 mm by fine-tuning the pinhole characteristics, the availability of longer-lived isotopes, and the high specific activity of most no-carrier-added SPECT tracers. Many PET tracers, particularly those labeled with ^{11}C, have a low specific activity which may lead to significant occupancy of the target site by the tracer itself to levels where there may be possible pharmacologic effects.

Recent developments of tumor-targeted SPECT radiotracers for imaging of cancer diseases has recently been reviewed in Müller and Schibli (2013), and considerations associated with tissue penetration, high affinity to the tumor-associated target structure, specific uptake and retention in the malignant lesions, and rapid clearance from nontargeted tissues and organs are addressed.

Examples of In-111 for larger (Abs) and Tc-99m for smaller molecules used in preclinical studies in oncology are many. One of the most advanced and exciting Tc-99m agents is that developed for folate imaging as part of a companion diagnostic package. Use of targeted therapy requires identification of patients whose tumors express a specific molecular target. Preclinical evaluation has been reported by Reddy et al. (2004). The folate receptor, which is over expressed by many primary and metastatic cancers, is an example of one system that can be successfully exploited for drug delivery. Folate-based radioligand labeled with In-111 was introduced and phase I/II clinical trials of In-111-diethylenetriaminepentaacetic acid-folate (In-111-DTPA-folate) were conducted in FR-positive ovarian cancers. However, plans to commercialize In-111-DTPA-folate were hampered by the high cost of In-111 and its suboptimal clinical applicability (i.e., long radiochemical half-life). Using a Tc-99m-folate conjugate, experiments were conducted to compare the biodistribution of intraperitoneal versus intravenous Tc-99m-EC20 and on the accessible targeting of both subcutaneous and intraperitoneal FR-positive tumors and to improve Tc-99m-EC20's TBR (tumor-to-blood ratio) co-injected versus pre-injected folic acid was also investigated. Preparation, radiochemical purity, yield, specific

activity, binding affinity, and tissue distribution studies were performed. Part of the qualification process in the preclinical models is to investigate differential levels of membrane-associated FR expression; 4T1, 4T1-pico, and M109 cells were used as tumor models for the assessment of Tc-99m-EC20 uptake; indeed net uptake of Tc-99m-EC20 in each of these tumors was proportional to their respective FR levels. Furthermore, FR-positive tumors are equally accessed by folate-targeted agents in a manner that is independent of both the tumor location and the route of dose administration. Nevertheless, many solid tumors have poorly formed vasculatures with intermittent blood flow and large distances between functional blood vessels and in the center of large tumors, increased interstitial pressure gradients cause radial fluid flow from the center to the periphery. Other factors, including foods (e.g., does the food or food metabolites contain competing products) and the critical mass of unlabeled peptide and the labeling specific activity (kBq/g), significantly affect uptake of peptide-based radioligands (Velikyan et al. 2008, 2010).

A major disadvantage of iodine-123 (I-123)-labeled monoclonal antibodies (MAbs) for SPECT imaging is the rapid diffusion of iodotyrosine from target cells after internalization and catabolism of the radioiodinated MAbs. In contrast, the chelated moieties remain intact longer in the systemic vasculature and are not subject to deiodination and offer a higher residualization. Indeed, assuring there is minimal metabolic processing of the radiolabeled product into radiolabeled subfragments (i.e., degradation) is the key consideration in reducing retention of antibodies (and confusing fragmentation) within the cell and reduces interpretive challenges of multiple product PK uptake, residency, and elimination profiles to the images (Shih et al. 1994).

Translation between SPECT and PET, for example, In-111 of DOTA-conjugated biological moieties can offer easier and cheaper data than that obtained by the PET equivalent trivalent ions. DOTA and DTPA avid SPECT radiometals (e.g., In-111) may be used for initial evaluation of a series of biological targeting moieties (BTMS; e.g., peptide, antibody, antibody fragments); once selection of an optimal BTM, the investigator may then move to the shorter-lived PET radioisotope. Anecdotal evidence suggests the distribution properties of the SPECT, and PET chelated radiometal may not greatly differ.

7.2.1.4 Computed Tomography (CT)

Like MRI, CT is often simply associated with anatomical imaging. Indeed, its use is most commonly identifying pathological lesions via alteration or distortion in normal structures. However, after administration of iodinated contrast agents—where conventionally this is used to enhance contrast (by absorption and attenuation of X-rays) in statically acquired images—more recently the i.v. administration of these agents can be followed with dynamic acquisitions where vascular hemodynamics and fine vascular structures related to flow impedance (atherosclerosis, etc.) can be resolved.

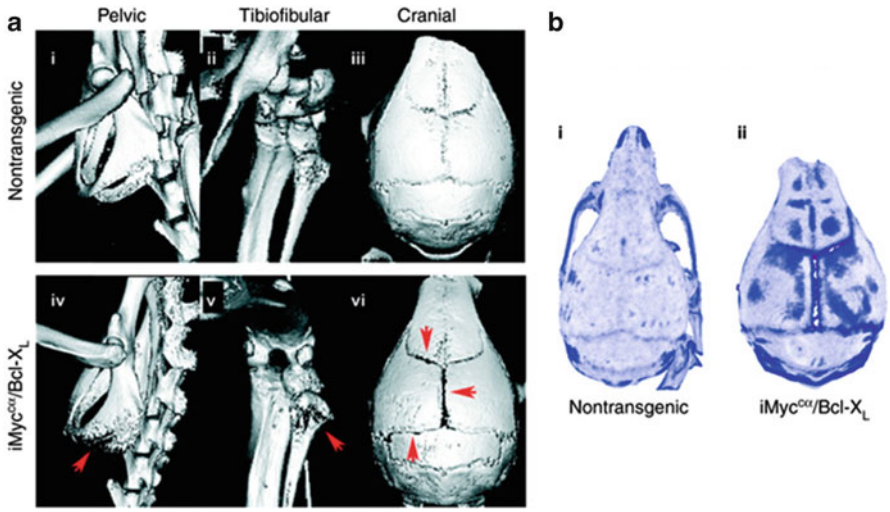

Fig. 7.5 (**a**) Osteolytic bone disease in the iMyc^{Cα}/Bcl-X$_L$ GEM model of de novo PCM. Unlike in age-matched nontransgenic (B6 × FVB/N) F$_1$ mice (*i–iii*), ex vivo CT imaging revealed evidence of osteolytic bone disease (*red arrows*) in the pelvic bone (*iv*), tibiofibular complex (*v*), and cranium (*vi*) of iMyc^{Cα}/Bcl-X$_L$ mice by approximately 110 days of age. (**b**) Increases in bone surface roughness and focal osteolytic lesions, which extended beyond the area of suture widening, were observed in 110-day-old iMyc^{Cα}/Bcl-X$_L$ mice (Lee et al. 2011b; with permissions)

CT uses X-rays to generate cross-sectional, two-dimensional images of the body. Images are acquired by rapid rotation of the X-ray tube a full 360° around the subject. The transmitted radiation is measured by a ring of sensitive radiation detectors located on the gantry around the subject.

Earlier publications of micro-CT in oncology animal models mainly explored skeletal changes associated with tumor dissemination and metastasis. A recent example was reported in complex GEMMS (http://www.ncbi.nlm.nih.gov/pubmed/15967710) models where spatial and temporal dynamics of lesion manifestation were unknown (Lee et al. 2011b). See Fig. 7.5 for a view of such distortion of bone from tumor invasion and displacement.

Like dynamic contrast enhanced-MRI (DCE-MRI), DCE-CT can offer parameters associated with hemodynamic constituents underlying vascular function in different disease states (e.g., atherosclerosis and tumors). Indeed, recently these two modalities have been compared in a rat tumor model (Ng et al. 2012). While both modalities had good reproducibility, their derived parameters were not equivalent. The latter could, in some part, be attributed to different sized molecular agents used and temporal resolution of the different modalities. However, other preclinical investigations have successfully used DCE-CT in the context of acute changes after antiangiogenic therapies (Cyran et al. 2012; Tai et al. 2010) (Fig. 7.6).

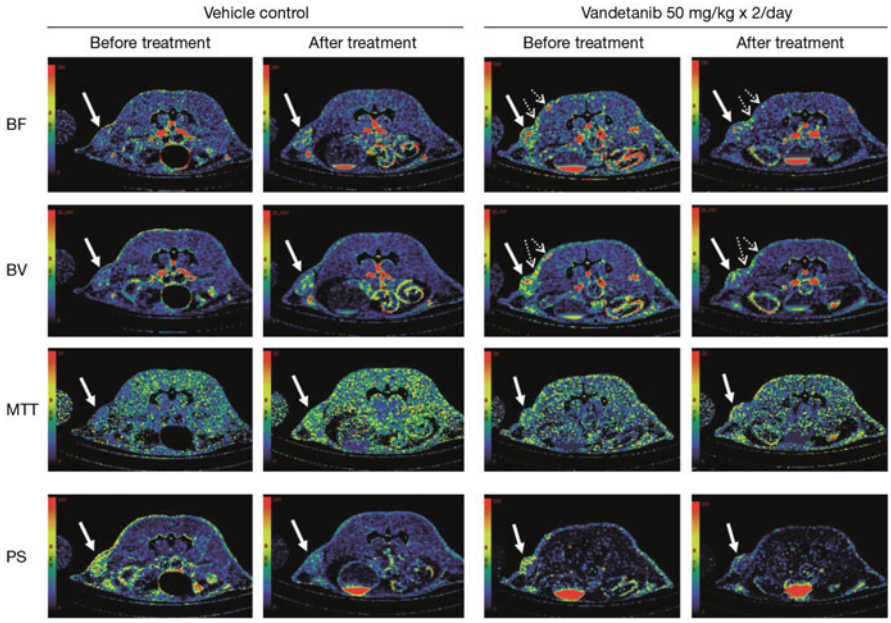

Fig. 7.6 Representative blood flow (BF), blood volume (BV), mean transit time (MTT), and permeability surface (PS) area maps of a transaxial section through the tumor of one vehicle- and one vandetanib-treated non-hypovascular tumor before and after treatment. In the BF, BV, MTT, and PS maps, values from 0 to 240 ml/min per 100 g, from 0 to 16 ml/100 g, from 0 to 20 s, and from 0 to 100 ml/min per 100 g, respectively, are coded according to the rainbow color scale. The parametric maps, in particular BF and BV, show the level of angiogenic activities in the tumor and adjacent tissue as indicated by *solid* and *dotted arrows* respectively (Images from Tai et al. (2010); with permission)

There are more CT cameras in clinical practice as stand-alone systems and as combined PET/CT systems versus combined or with MRI systems, and this is in part the motivation for preclinical studies with CT as the translational possibilities are perhaps greater than that with DCE-MRI. However, the CT radiation risk (Brenner and Hall 2007) in humans that exists is far greater when dynamic data is acquired compared to static acquisitions. Although methods are being introduced to reduce radiation exposure (*Image Gently*™ program out of the SNMI), the impact on sensitivity to hemodynamic changes has still to be determined (Kim et al. 2011). Limited literature exists for animal studies and the risks of radiation exposure from CT scans (Boone et al. 2004), but careful consideration is recommended in longitudinal studies (Willekens et al. 2010; Kersemans et al. 2011b) as these protocols are intended to be translated to human clinical use and radiation risk must be considered.

Multimodality has not been described in this chapter; however, PET/CT and SPECT/CT are the major multimodal techniques applied in preclinical oncology (Kapoor et al. 2004). Fundamentally, the combination of functional/molecular

Table 7.1 Names and intended physiologic targets of PET tracers[a] often used in clinical oncology and in laboratory studies using small animals are listed (Smith et al. 2012)

^{18}F FDG	Glucose metabolism/localization
3-F-18 Fluoro-3-deoxythymidine	Tumor proliferation
^{11}C Choline/^{18}F fluorocholine	Choline metabolism
^{18}F Fluoro-L-DOPA	Neuroendocrine tumors
^{18}F Fluoroethyltyrosine	Amino acid transport
^{18}F AH111585 (F18 fluciclatide)	Angiogenesis
^{18}F FACBC	Amino acid transport
^{18}F FMISO	Hypoxia
^{18}F HX4	Hypoxia
^{18}F EF5	Hypoxia
^{64}Cu ATSM	Hypoxia
^{68}Ga DOTATATE	Neuroendocrine tumors
^{18}F FES	Estrogen receptor
^{18}F RGD-K5	Angiogenesis
^{68}Ga BNOTA-PRGD2	Angiogenesis
^{18}F Paclitaxel	Multidrug resistance
^{89}Zr Bevacizumab	VEGF
^{18}F VM4-037	Carbonic anhydrase IX
^{89}Zr Cetuximab	EGFR
^{18}F FFNP	Progesterone receptor
^{64}Cu DOTA-U3-1287	HER3
^{18}F BAY94-9392	Amino acid transport
^{124}I NM404	Brain glioma
^{124}I cG250	Carbonic anhydrase IX
^{18}F ML-10	Apoptosis
^{11}C Lapatinib	Her2
^{18}F Annexin V	Apoptosis
^{18}F FAC	Tumor proliferation
^{11}C Verapamil	P-gp expression

The reader is encouraged to review the appropriateness of each agent, particularly biologics, which may exhibit species specificity in target binding in an animal system

[a]This list is not intended to be exhaustive and many agents are continuing to be added to this list

imaging with anatomical registration enables the investigator to work with high confidence in advanced disease models, e.g., orthotopic or genetically engineered mouse models with spontaneous lesion development. Beyond these is the recent introduction of PET/MRI (Cherry 2009). The latter has recently overcome some exquisite engineering complications associated with PET-associated electronics operating under conditions of high magnetic fields while still retaining spatial resolution and quantification capabilities.

7.2.1.5 Radiotracers/Radiopharmaceuticals ("Tracers")

The reader is encouraged to review this section with added information from the National Library of Medicine regarding radiotracers (ref: http://www.ncbi.nlm.nih.gov/books/NBK5330/). Table 7.1 describes several radiotracers created for PET imaging.

7.3 Animal Models Useful in Cancer Therapeutic Development

The reader is encouraged to examine a general review of the animal models used in cancer research over the years; see Frese and Tuveson (2007) and the earlier paper of Marx (2003).

In oncology preclinical studies, the most common publication of data when new targeted therapeutics are presented is the chemical structure of the new molecule, binding data from in vitro IC50s in multiple cell lines, and a mechanism of action treatise on how the molecule performs in vivo in these different lines as subcutaneous (SC) xenograft masses studied on the flank of immunocompromised species and other murine strains of choice. The SC xenograft efficacy protocol is typically represented by short-term (~21 days) tumor growth kinetics measured with calipers in three axial directions creating a tumor mass volume estimate. The treated arms of studies are compared to a standard-of-care and vehicle treatment, and the "tumor versus control" response metrics (size, orientation, visual appearance, etc.) are reported. Much criticism has been laid upon the ATCC SC xenograft models approach as there has been actually limited predictability realized to date for translational therapeutic efficacy and even for a translational basis of drug exposure (Johnson et al. 2001). The inherent "homogeneity" of the xenograft cells and the lack of the "normal" stromal and vascular component architectures at the onset make the xenograft models somewhat questionable for modeling the in situ nidus of tumor development. However, results from Voskoglou-Nomikos et al. (2003) suggest under the right conditions and when multiple models or tumor panels are used, these models may be useful in predicting the phase II clinical trial efficacy performance of cancer drugs and biologics.

Syngeneic cells benefit from being able to be used in animals whose immune system remains intact, and that this kind of cell system can play a large part in making a tumor response clinically relevant. The models are to date limited and the argument is that one is treating rat or mouse cancer cells and that the mutations may not be preserved or activated/inhibited in a manner similar to that of the human equivalent malignancy (de Jong and Maina 2010). It is imperative we always remember we are dealing with "models" and that there will be intrinsic differences from the human clinical experience that must be considered.

However, for qualifying imaging biomarkers in the context of a pharmaceutically targeted agent, if one can presume the mechanism of action (MoA) of these agents

is preserved through to the intended clinical population, then these models add value. For example, DCE-MRI systems, a measurement used to confirm acute hemodynamic changes after antiangiogenic treatments, have been useful preclinically and clinically in a number of cases. While only anecdotal, the changes observed in syngeneic lines or SC xenografts using the same type of contrast agents and similar acquisition routines appear to match that observed in a clinical context. In support of this, we first see that Lee et al. (2006) observed the reduction in tumor vascularity correlated significantly with improved clinical outcomes in patients with advanced colorectal cancer and liver metastases. They went onto assess the biomarkers used in the clinical trials and applied these markers in an orthotopic, syngeneic mouse model: C57BL/6 mice injected in the ear pinnae with murine B16/BL6 melanoma cells which metastases to the cervical lymph nodes; a change from baseline in the MRI-measured DCE-MRI parameter for the B16/BL6 melanoma model after treatment with PTK/ZK appeared to correlate well with antitumor activity of the agent. Through PK/PD modeling of the mouse B16/BL6 melanoma model MRI-initial area under the curve measures appear to be predictive of both tumor response and the pharmacodynamic effects of PTK/ZK in patients at equivalent drug exposures (Lee et al. 2006). Secondly, in two SC xenograft models Lovo (human colorectal carcinoma) or C6 (rat glioma) tumors, treated with Cediranib (RECENTIN, AZD2171), a highly potent inhibitor of the tyrosine kinase activity associated with all three vascular endothelial growth factor (VEGF) receptors, and imaged with DCE-MRI at baseline and 2 h after the final dose (3 doses, given at 2, 26, and 50 h), showed acute changes in two DCE-MRI parameters (Bradley et al. 2009), and these observations could be translated to that observed in the phase I clinical study of AZD2171 in patients with advanced solid tumors (Drevs et al. 2007). The observations revealed pharmacodynamic time-, dose-, and exposure-related decreases in the initial area under the curve, again defined as the DCE-MRI data collected over 60 s post-contrast arrival in the tissue (i.e., iAUC60).

Patient-derived xenografts (PDX), where fresh surgical tumor tissue is obtained and implanted subcutaneously or orthotopically in mice, are emerging as a new addition to the battery of preclinical models to test targeted agents. PDX are thought to more faithfully recapitulate the molecular diversity, cellular heterogeneity, and histology seen in patient tumors albeit the issues described earlier of actual tissue initiation. Differences in targeted therapy response rates between patient-derived tumor tissue and xenografts have been observed (Jin et al. 2012). However, limitations do exist and must be considered in the context of availability of other preclinical models (Kopetz et al. 2012). Limited literature exists where imaging PDX is specifically described (Germanos 2011, WMIC Abs P779).

Xenografts, syngeneic cell lines, and PDX can be inoculated orthotopically; this mode of implantation is more complex but may better recapitulate the microenvironment of what may be expected in the clinical context, e.g., stromal infiltration and delivery barriers of therapy as well as nutrients and vascular access. Extensive literature exists where imaging of orthotopically implanted tumors has revealed response to treatment using noninvasive measurements. Hoff et al. (2012) showed

the utility of simultaneously acquiring DCE- and DW-MRI data in an orthotopically implanted model of glioma; imaging pre- and post-VEGF-Trap (aka., Aflibercept) treatment showed acute changes in both DCE as well as DW derived parameters that were corroborated by histopathological findings. Furthermore, the impact of tumor growth on the tumor implantation sites were examined by Zechmann et al. (2007) where DCE-MRI and ^{1}H-MRS were assessed and compared between the two sites (orthotopic vs. subcutaneous); indeed, some tumor lines show comparable parameter changes and some are different.

Emerging data suggests that genetically engineered mouse model systems (GEMMS) better predict therapeutic responses and PK than the more traditional xenograft tumor systems (Chesi et al. 2012; Combest et al. 2012). Furthermore, Yuneva et al. (2012) have shown that the metabolic profile of the tumor depends on both the genetic lesion and tissue type. A most comprehensive assessment of a GEMM was by (Chen et al. 2012); understanding that while patients are often stratified by a single oncogenic driver mutation, the impact of coexisting genetic mutations, especially the loss of tumor suppressors, had not yet been fully explored. Comparison of F-18-FDG avidity, quantified by the standardized uptake value (SUV) calculation in lung cancers across three different genotypes showed an overall higher FDG uptake in both KRAS/p53 and KRAS/Lkb1 tumors compared to simple KRAS tumors alone. Expression of the glucose transporter GLUT1 was elevated in KRAS/Lkb1 mutant tumors, consistent with an increased baseline FDG-PET SUV signal. To determine if this finding was applicable to human patients, FDG avidity in nine patients with KRAS-mutated lung cancer was examined (Yuneva et al. 2012). Tumors from three patients positive for LKB1 immunostaining had a mean maximum SUV (SUV_{max}) of 2.33, whereas tumors from six patients negative for LKB1 immunostaining had a mean SUV_{max} of 8.75, a near fourfold difference.

7.4 Summary

In conclusion, biomedical imaging is becoming an integral biomarker in drug discovery and development. As illustrated in this chapter, the different modalities can reveal functional and physiological parameters otherwise unattainable by conventional methods. These measurements can be used when new animal models are developed and to follow acute pharmacodynamic changes during drug treatment. Furthermore, translational science (“bench to bedside”) and the use of clinically relevant modalities and appropriate clinical endpoints allow the researcher to qualify a novel/conventional biomarker in a selected preclinical model and, assuming preservation of MoA of the therapy, allow for the development of novel drug entities which can be utilized in their respective clinical oncology scenarios with the same expected targeting and tumor outcomes using the model-defined imaging techniques.

References

Aboagye EO (2005) Positron emission tomography imaging of small animals in anticancer drug development. Mol Imaging Biol 7:53–58

Albanese C, Rodriguez OC, Vanmeter J, Fricke ST, Rood BR, Lee Y, Wang SS, Madhavan S, Gusev Y, Petricoin EF, 3rd, et al (2012) Preclinical magnetic resonance imaging and systems biology in cancer research: Current applications and challenges. Am J Pathol

Bahce I, Smit EF, Lubberink M, van der Veldt AA, Yaqub M, Windhorst AD, Schuit RC, Thunnissen E, Heideman DAH, Postmus PE et al (2013) Development of [11C]erlotinib positron emission tomography for in vivo evaluation of epidermal growth factor receptor mutational status. Clin Cancer Res Off J Am Assoc Cancer Res 19:183–193

Barnes SL, Whisenant JG, Loveless ME, Yankeelov TE (2012) Practical dynamic contrast enhanced MRI in small animal models of cancer: data acquisition, data analysis, and interpretation. Pharmaceutics 4:442–478

Baudelet C, Gallez B (2004) Effect of anesthesia on the signal intensity in tumors using BOLD-MRI: comparison with flow measurements by Laser Doppler flowmetry and oxygen measurements by luminescence-based probes. Magn Reson Imaging 22:905–912

Boone JM, Velazquez O, Cherry SR (2004) Small-animal X-ray dose from micro-CT. Mol Imaging 3:149–158

Bradley DP, Tessier JJ, Lacey T, Scott M, Jürgensmeier JM, Odedra R, Mills J, Kilburn L, Wedge SR (2009) Examining the acute effects of cediranib (RECENTIN, AZD2171) treatment in tumor models: a dynamic contrast-enhanced MRI study using gadopentate. Magn Reson Imaging 27:377–384

Breeman WAP, De Blois E, Sze Chan H, Konijnenberg M, Kwekkeboom DJ, Krenning EP (2011) (68)Ga-labeled DOTA-peptides and (68)Ga-labeled radiopharmaceuticals for positron emission tomography: current status of research, clinical applications, and future perspectives. Semin Nucl Med 41:314–321

Brenner DJ, Hall EJ (2007) Computed tomography — an increasing source of radiation exposure. N Engl J Med 357:2277–2284

Buchmann I, Henze M, Engelbrecht S, Eisenhut M, Runz A, Schäfer M, Schilling T, Haufe S, Herrmann T, Haberkorn U (2007) Comparison of 68Ga-DOTATOC PET and 111In-DTPAOC (Octreoscan) SPECT in patients with neuroendocrine tumours. Eur J Nucl Med Mol Imaging 34:1617–1626

Chen Z, Cheng K, Walton Z, Wang Y, Ebi H, Shimamura T, Liu Y, Tupper T, Ouyang J, Li J et al (2012) A murine lung cancer co-clinical trial identifies genetic modifiers of therapeutic response. Nature 483:613–617

Cherry SR (2009) Multimodality imaging: beyond PET/CT and SPECT/CT. Semin Nucl Med 39:348–353

Chesi M, Matthews GM, Garbitt VM, Palmer SE, Shortt J, Lefebure M, Stewart AK, Johnstone RW, Bergsagel PL (2012) Drug response in a genetically engineered mouse model of multiple myeloma is predictive of clinical efficacy. Blood 120:376–385

Combest AJ, Roberts PJ, Dillon PM, Sandison K, Hanna SK, Ross C, Habibi S, Zamboni B, Müller M, Brunner M et al (2012) Genetically engineered cancer models, but not xenografts, faithfully predict anticancer drug exposure in melanoma tumors. Oncologist 17:1303–1316

Cyran CC, Von Einem JC, Paprottka PM, Schwarz B, Ingrisch M, Dietrich O, Hinkel R, Bruns CJ, Clevert DA, Eschbach R et al (2012) Dynamic contrast-enhanced computed tomography imaging biomarkers correlated with immunohistochemistry for monitoring the effects of sorafenib on experimental prostate carcinomas. Invest Radiol 47:49–57

de Jong M, Maina T (2010) Of mice and humans: are they the same?—implications in cancer translational research. J Nucl Med 51:501–504

Doty FD, Entzminger G, Kulkarni J, Pamarthy K, Staab JP (2007) Radio frequency coil technology for small-animal MRI. NMR Biomed 20:304–325

Drevs J, Siegert P, Medinger M, Mross K, Strecker R, Zirrgiebel U, Harder J, Blum H, Robertson J, Jürgensmeier JM et al (2007) Phase I clinical study of AZD2171, an oral vascular endothelial growth factor signaling inhibitor, in patients with advanced solid tumors. J Clin Oncol 25: 3045–3054

Ebenhan T, Honer M, Ametamey SM, Schubiger PA, Becquet M, Ferretti S, Cannet C, Rausch M, McSheehy PMJ (2009) Comparison of [18F]-tracers in various experimental tumor models by PET imaging and identification of an early response biomarker for the novel microtubule stabilizer patupilone. Mol Imaging Biol 11:308–321

Ferris CF, Smerkers B, Kulkarni P, Caffrey M, Afacan O, Toddes S, Stolberg T, Febo M (2011) Functional magnetic resonance imaging in awake animals. Rev Neurosci 22:665–674

Firestone B (2010) The challenge of selecting the "right" in vivo oncology pharmacology model. Curr Opin Pharmacol 10:391–396

Franc BL, Acton PD, Mari C, Hasegawa BH (2008) Small-animal SPECT and SPECT/CT: important tools for preclinical investigation. J Nucl Med 49:1651–1663

Frese KK, Tuveson DA (2007) Maximizing mouse cancer models. Nat Rev Cancer 7:645–658

Germanos M (2011) In vivo longitudinal 2-deoxy-2-[18F]fluoro-D-glucose (FDG) PET characterization of primary human tumor explant xenografts in mice. World Molecular Imaging Congress P779

Groch MW, Erwin WD (2000) SPECT in the year 2000: basic principles. J Nucl Med Technol 28:233–244

Hanahan D, Weinberg RA (2011) Hallmarks of cancer: the next generation. Cell 144:646–674

Heijmen L, Ter Voert EEGW, Nagtegaal ID, Span P, Bussink J, Punt CJA, de Wilt JHW, Sweep FCGJ, Heerschap A, van Laarhoven HWM (2013) Diffusion-weighted MR imaging in liver metastases of colorectal cancer: reproducibility and biological validation. Eur Radiol 23: 748–756

Hodkinson DJ, De Groote C, McKie S, Deakin JFW, Williams SR (2012) Differential effects of anaesthesia on the phMRI response to acute ketamine challenge. Br J Med Med Res 2: 373–385

Hoff BA, Bhojani MS, Rudge J, Chenevert TL, Meyer CR, Galbán S, Johnson TD, Leopold JS, Rehemtulla A, Ross BD et al (2012) DCE and DW-MRI monitoring of vascular disruption following VEGF-Trap treatment of a rat glioma model. NMR Biomed 25:935–942

Jin K, Lan H, Cao F, Han N, Xu Z, Li G, He K, Teng L (2012) Differential response to EGFR- and VEGF-targeted therapies in patient-derived tumor tissue xenograft models of colon carcinoma and related metastases. Int J Oncol 41:583–588

Johnson JI, Decker S, Zaharevitz D, Rubinstein LV, Venditti JM, Schepartz S, Kalyandrug S, Christian M, Arbuck S, Hollingshead M et al (2001) Relationships between drug activity in NCI preclinical in vitro and in vivo models and early clinical trials. Br J Cancer 84:1424–1431

Jones T (1996) The imaging science of positron emission tomography. Eur J Nucl Med 23: 807–813

Kapoor V, McCook BM, Torok FS (2004) An introduction to PET-CT imaging1. Radiographics 24:523–543

Kersemans V, Cornelissen B, Hueting R, Tredwell M, Hussien K, Allen PD, Falzone N, Hill SA, Dilworth JR, Gouverneur V et al (2011a) Hypoxia imaging using PET and SPECT: the effects of anesthetic and carrier gas on [Cu]-ATSM, [Tc]-HL91 and [F]-FMISO tumor hypoxia accumulation. PLoS One 6:e25911

Kersemans V, Thompson J, Cornelissen B, Woodcock M, Allen PD, Buls N, Muschel RJ, Hill MA, Smart SC (2011b) Micro-CT for anatomic referencing in PET and SPECT: radiation dose, biologic damage, and image quality. J Nucl Med 52:1827–1833

Kim SM, Haider MA, Milosevic M, Jaffray DA, Yeung IWT (2011) A method for patient dose reduction in dynamic contrast enhanced CT study. Med Phys 38:5094–5103

Kinahan PE, Fletcher JW (2010) PET/CT standardized uptake values (SUVs) in clinical practice and assessing response to therapy. Semin Ultrasound CT MR 31:496–505

Knowles SM, Wu AM (2012) Advances in immuno-positron emission tomography: antibodies for molecular imaging in oncology. J Clin Oncol 30:3884–3892

Kopetz S, Lemos R, Powis G (2012) The promise of patient-derived xenografts: the best laid plans of mice and men. Clin Cancer Res Off J Am Assoc Cancer Res 18:5160–5162

Lee L, Sharma S, Morgan B, Allegrini P, Schnell C, Brueggen J, Cozens R, Horsfield M, Guenther C, Steward WP et al (2006) Biomarkers for assessment of pharmacologic activity for a vascular endothelial growth factor (VEGF) receptor inhibitor, PTK787/ZK 222584 (PTK/ZK): translation of biological activity in a mouse melanoma metastasis model to phase I studies in patients with advanced colorectal cancer with liver metastases. Cancer Chemother Pharmacol 57:761–771

Lee E, Kamlet AS, Powers DC, Neumann CN, Boursalian GB, Furuya T, Choi DC, Hooker JM, Ritter T (2011a) A fluoride-derived electrophilic late-stage fluorination reagent for PET imaging. Science 334:639–642

Lee EC, Fitzgerald M, Bannerman B, Donelan J, Bano K, Terkelsen J, Bradley DP, Subakan O, Silva MD, Liu R et al (2011b) Antitumor activity of the investigational proteasome inhibitor MLN9708 in mouse models of B-cell and plasma cell malignancies. Clin Cancer Res 17: 7313–7323

Marx J (2003) Building better mouse models for studying cancer. Science 299:1972–1975

McArthur GA, Puzanov I, Amaravadi R, Ribas A, Chapman P, Kim KB, Sosman JA, Lee RJ, Nolop K, Flaherty KT et al (2012) Marked, homogeneous, and early [18F]fluorodeoxyglucose-positron emission tomography responses to vemurafenib in BRAF-mutant advanced melanoma. J Clin Oncol 30:1628–1634

McGrath DM, Bradley DP, Tessier JL, Lacey T, Taylor CJ, Parker GJM (2009) Comparison of model-based arterial input functions for dynamic contrast-enhanced MRI in tumor bearing rats. Magn Reson Med 61:1173–1184

Memon AA, Jakobsen S, Dagnaes-Hansen F, Sorensen BS, Keiding S, Nexo E (2009) Positron emission tomography (PET) imaging with [11C]-labeled erlotinib: a micro-PET study on mice with lung tumor xenografts. Cancer Res 69:873–878

Morse DL, Gillies RJ (2010) Molecular imaging and targeted therapies. Biochem Pharmacol 80: 731–738

Müller C, Schibli R (2013) Single photon emission computed tomography tracer. Recent Results Cancer Res 187:65–105

Neil JJ (2008) Diffusion imaging concepts for clinicians. J Magn Reson Imaging 27:1–7

Nelson GS, Perez J, Colomer MV, Ali R, Graves E (2011) Facilitating multimodal preclinical imaging studies in mice by using an immobilization bed. Comp Med 61:499–504

Ng CS, Waterton JC, Kundra V, Brammer D, Ravoori M, Han L, Wei W, Klumpp S, Johnson VE, Jackson EF (2012) Reproducibility and comparison of DCE-MRI and DCE-CT perfusion parameters in a rat tumor model. Technol Cancer Res Treat 11:279–288

Nguyen Q-D, Perumal M, Waldman TA, Aboagye EO (2011) Glucose metabolism measured by [^{18}F]fluorodeoxyglucose positron emission tomography is independent of PTEN/AKT status in human colon carcinoma cells. Transl Oncol 4:241–248

Ou S-HI, Bartlett CH, Mino-Kenudson M, Cui J, Iafrate AJ (2012) Crizotinib for the treatment of ALK-rearranged non-small cell lung cancer: a success story to usher in the second decade of molecular targeted therapy in oncology. Oncologist 17:1351–1375

Pantaleo MA, Nicoletti G, Nanni C, Gnocchi C, Landuzzi L, Quarta C, Boschi S, Nannini M, Di Battista M, Castellucci P et al (2010) Preclinical evaluation of KIT/PDGFRA and mTOR inhibitors in gastrointestinal stromal tumors using small animal FDG PET. J Exp Clin Cancer Res 29:173

Padhani AR, Liu G, Mu-Koh D, Chenevert TL, Thoeny HC, Takahara T, Dzik-Jurasz A, Ross BD, Van Cauteren M, Collins D et al (2009) Diffusion-Weighted magnetic resonance imaging as a cancer biomarker: consensus and recommendations. Neoplasia 11:102–125

Pautler RG (2004) Mouse MRI: concepts and applications in physiology. Physiology (Bethesda) 19:168–175

Pysz MA, Gambhir SS, Willmann JK (2010) Molecular imaging: current status and emerging strategies. Clin Radiol 65:500–516

Reddy JA, Xu L-C, Parker N, Vetzel M, Leamon CP (2004) Preclinical evaluation of (99m) Tc-EC20 for imaging folate receptor-positive tumors. J Nucl Med 45:857–866

Schnell C, Arnal S, Barbé S, Becquet M, Garcia-Echeverria C, Cozens R (2010) 261 Effects of isoflurane anesthesia on bioluminescence measurements: impact on pharmacological assessment of anti-tumor activity of chemical entities. Eur J Cancer Supplements 8:85

Seo Y, Jiang H, Franc BL (2013) Preclinical SPECT and SPECT/CT. Recent Results Cancer Res 187:193–220

Serkova NJ, Spratlin JL, Eckhardt SG (2007) NMR-based metabolomics: translational application and treatment of cancer. Curr Opin Mol Ther 9:572–585

Shih LB, Thorpe SR, Griffiths GL, Diril H, Ong GL, Hansen HJ, Goldenberg DM, Mattes MJ (1994) The processing and fate of antibodies and their radiolabels bound to the surface of tumor cells in vitro: a comparison of nine radiolabels. J Nucl Med 35:899–908

Smith TB, Nayak KS (2010) MRI artifacts and correction strategies. Imaging Med 2(4):445–457

Smith G, Carroll L, Aboagye EO (2012) New frontiers in the design and synthesis of imaging probes for PET oncology: current challenges and future directions. Mol Imaging Biol 14: 653–666

Spratlin JL, Serkova NJ, Eckhardt SG (2009) Clinical applications of metabolomics in oncology: a review. Clin Cancer Res 15:431–440

Tai JH, Tessier J, Ryan AJ, Hoffman L, Chen X, Lee T-Y (2010) Assessment of acute antivascular effects of vandetanib with high-resolution dynamic contrast-enhanced computed tomographic imaging in a human colon tumor xenograft model in the nude rat. Neoplasia 12:697–707

Therasse P, Eisenhauer EA, Verweij J (2006) RECIST revisited: a review of validation studies on tumour assessment. Eur J Cancer 42:1031–1039

Velikyan I, Beyer GJ, Bergström-Pettermann E, Johansen P, Bergström M, Långström B (2008) The importance of high specific radioactivity in the performance of 68Ga-labeled peptide. Nucl Med Biol 35:529–536

Velikyan I, Sundin A, Eriksson B, Lundqvist H, Sörensen J, Bergström M, Långström B (2010) In vivo binding of [68Ga]-DOTATOC to somatostatin receptors in neuroendocrine tumours–impact of peptide mass. Nucl Med Biol 37:265–275

Verel I, Visser GWM, Boellaard R, Stigter-van Walsum M, Snow GB, Van Dongen GAMS (2003) 89Zr immuno-PET: comprehensive procedures for the production of 89Zr-labeled monoclonal antibodies. J Nucl Med 44:1271–1281

Vincent MD, Kuruvilla MS, Leighl NB, Kamel-Reid S (2012) Biomarkers that currently affect clinical practice: EGFR, ALK, MET, KRAS. Curr Oncol 19:S33–S44

Voskoglou-Nomikos T, Pater JL, Seymour L (2003) Clinical predictive value of the in vitro cell line, human xenograft, and mouse allograft preclinical cancer models. Clin Cancer Res 9: 4227–4239

Willekens I, Buls N, Lahoutte T, Baeyens L, Vanhove C, Caveliers V, Deklerck R, Bossuyt A, De Mey J (2010) Evaluation of the radiation dose in micro-CT with optimization of the scan protocol. Contrast Media Mol Imaging 5:201–207

Yim H, Seo S, Na K (2011) MRI contrast agent-based multifunctional materials: diagnosis and therapy. J Nanomater 11 page

Yuneva MO, Fan TWM, Allen TD, Higashi RM, Ferraris DV, Tsukamoto T, Matés JM, Alonso FJ, Wang C, Seo Y et al (2012) The metabolic profile of tumors depends on both the responsible genetic lesion and tissue type. Cell Metab 15:157–170

Zechmann CM, Woenne EC, Brix G, Radzwill N, Ilg M, Bachert P, Peschke P, Kirsch S, Kauczor H-U, Delorme S et al (2007) Impact of stroma on the growth, microcirculation, and metabolism of experimental prostate tumors. Neoplasia 9:57–67

Zieba A, Grannas K, Söderberg O, Gullberg M, Nilsson M, Landegren U (2012) Molecular tools for companion diagnostics. N Biotechnol 29:634–640